

NAR Breakthrough Article

Engineering large-scale chromosomal deletions by CRISPR-Cas9

Thomas F. Eleveld^{1,*}, Chaimaa Bakali¹, Paul P. Eijk¹, Phylcia Stathi¹, Lianne E. Vriend², Pino J. Poddighe² and Bauke Ylstra¹

¹Department of Pathology, Cancer Center Amsterdam, Amsterdam UMC, Vrije Universiteit Amsterdam, De Boelelaan 1117, 1081 HV Amsterdam, the Netherlands and ²Department of Clinical Genetics, Amsterdam UMC, Vrije Universiteit Amsterdam, De Boelelaan 1117, 1081 HV Amsterdam, the Netherlands

Received March 29, 2021; Revised June 07, 2021; Editorial Decision June 08, 2021; Accepted June 14, 2021

ABSTRACT

Large-scale chromosomal deletions are a prevalent and defining feature of cancer. A high degree of tumor-type and subtype specific recurrences suggest a selective oncogenic advantage. However, due to their large size it has been difficult to pinpoint the oncogenic drivers that confer this advantage. Suitable functional genomics approaches to study the oncogenic driving capacity of large-scale deletions are limited. Here, we present an effective technique to engineer large-scale deletions by CRISPR-Cas9 and create isogenic cell line models. We simultaneously induce double-strand breaks (DSBs) at two ends of a chromosomal arm and select the cells that have lost the intermittent region. Using this technique, we induced large-scale deletions on chromosome 11q (65 Mb) and chromosome 6q (53 Mb) in neuroblastoma cell lines. A high frequency of successful deletions (up to 30% of selected clones) and increased colony forming capacity in the 11q deleted lines suggest an oncogenic advantage of these deletions. Such isogenic models enable further research on the role of large-scale deletions in tumor development and growth, and their possible therapeutic potential.

INTRODUCTION

Somatic genetic alterations, like mutations, translocations and copy number changes, are the driving force of cancer, involved in not only oncogenesis but also tumor evolution and progression, therapy sensitivity and resistance (1). Genetic alterations are tumor type and even subtype specific

and determine their malignant potential. Functional genomics is a mainstay to comprehensively study the role of the genetic alterations to explain tumor development and growth.

Gene specific mutations have given a lot of insight into the oncogenic processes driving certain cancer types. For a variety of such mutations these studies have led to clinically effective treatment modalities that directly inhibit the function of the mutant proteins, such as the use of specific BRAF inhibitors in tumors with *BRAF* mutations (2). Translocations that recurrently affect particular genes are relatively easily modeled and have therefore been extensively studied. For several translocations this has also led to precision medication that targets the fusion protein, like Imatinib for tumors that harbor the BCR-ABL oncogene (3). Copy number changes come in a large size range from focal events, affecting small regions of up to 3 MB with one or few genes, to entire chromosomes, chromosomal arms or large parts thereof, affecting hundreds to thousands of genes (4). For recurrent focal chromosomal copy number aberrations the driving genes are also relatively easily identified, exposing strong driving oncogenes and tumor suppressor genes (5), and also in some cases other functional elements like microRNAs (6). Several of these can also be targeted by specific inhibitors, leading to significant clinical benefit, like for the use of Herceptin for HER2 amplified cancers (7). For most recurrent large-scale chromosomal aberrations, however, the large number of genes and regulatory elements affected complicates the elucidation of the underlying oncogenic processes. Subsequently, no targeted medicine is available yet that targets large-scale copy number aberrations.

Large-scale chromosomal copy number aberrations can be highly recurrent, with the most frequent events, like 8p loss, 17p loss and 8q gain, occurring in >30% of solid malignancies.

*To whom correspondence should be addressed. Tel +31 20 4442495; Email: t.f.eleveld@prinsesmaximacentrum.nl
Present address: Thomas F. Eleveld, Looijenga Group, Princess Maxima Centre for Pediatric Oncology, Heidelberglaan 25, 3584 CS Utrecht.

nancies (8). Large-scale events affect a vastly larger number of genes than other genomic changes (mutations, translocation, focal events), but each gene to a much smaller extent. This observation, combined with the paucity of clear driving genes or regulatory elements behind these large-scale changes, has led to the suggestion that large-scale aberrations could possibly promote tumor growth not by affecting the function of a single driver, but by concerted regulation of multiple genes and regulatory elements located on the involved region (9,10)

The molecular function of most established oncogenes and tumor suppressor genes has been extensively studied through the use of functional genetic experiments in relevant model systems (knockdown, knockout, overexpression etc.). However, very little is known about the functional effects of large-scale chromosomal copy number aberrations, since it is difficult to study the effects of subtle changes in the expression of multiple genes by conventional molecular biology approaches. The few studies that have addressed this subject have shown counterintuitive results, demonstrating that gain of single chromosomes is associated with a tumor-suppressive rather than tumor-promoting effect (11,12).

Here, we present a technique to induce large chromosomal deletions using CRISPR/Cas9 by simultaneously introducing double strand breaks (DSBs) at two locations within one chromosomal arm and a synthetic single-stranded DNA (ssDNA) template that spans the created gap for repair. Using this protocol, large-scale deletions that are observed in patients and are associated with poor prognosis are introduced in neuroblastoma cell lines. Neuroblastoma tumors contain relatively few mutations (13), while they do show highly recurrent chromosomal aberrations, some of which are strongly associated with poor prognosis (14,15). This suggests that these chromosomal aberrations have a tumor driving role and that neuroblastoma cells are a suitable model system to study the underlying mechanisms. Terminal deletions on chromosome 11q (65Mb) and 6q (53 Mb), were modeled by making double strand breaks and inducing translocations between sites where deletions were recurrently observed in patients, and the telomere of the targeted chromosome, with up to 30% of clones containing the desired deletion. With this technique, we offer a method for the generation of isogenic model systems of large-scale chromosomal deletions.

MATERIALS AND METHODS

Cell culture

Cell lines were cultured in DMEM supplemented with 10% FCS, 20 mM L-glutamine, 10 U/ml penicillin and 10 µg/ml streptomycin and maintained at 37°C under 5% CO₂. Cell line identities were regularly confirmed by short tandem repeat (STR) profiling using the PowerPlex16 system and GeneMapper software (Promega) (16). Cell lines were regularly screened for mycoplasma.

Colony formation assay

Single cell suspensions of deletion-positive and deletion-negative clones were seeded into six-well plates (2 × 10⁴ cells/well). At the endpoints of colony formation assays,

Table 1A. crRNAs used in this study

| | |
|-----------------|-----------------------|
| 11q Centromeric | GGTCAAACCTGGTACAGTTG |
| 11q Telomeric | CGATAACCAAGTGGCAGACG |
| 6q Centromeric | CATTGGTGCCCAACTGTTA |
| 6q Telomeric | ATCTGAATTAACACCATAACC |

Table 1B. Primers used in this study

| | |
|-------|------------------------|
| 11Q_A | GGAAAGATGCCACACAGTCCT |
| 11Q_B | GGAGATAATGCTTGGGCTGTC |
| 11Q_C | AAGGAAGGCAATTCACGGAAG |
| 11Q_D | GGATTCAGGGTCTCTCCTTGC |
| 11Q_E | GCCTCAGAGCAGGAACAGTACA |
| 6Q_A | GCCCTTAAATGCTGTACAAA |
| 6Q_B | GCTGCATCTTCTTCTTCTGC |
| 6Q_C | GTCTTCTGCACTTGGCAAAC |

cells were fixed, stained with crystal violet and scanned. All clones of each cell line were fixed at the same time. Scans of all wells were quantified using ImageJ software (17).

RNP complexes and transfection

Custom crRNA's, tracrRNA and recombinant Cas9 protein were acquired from Integrated DNA Technologies. The sequences for the crRNA's are shown in Table 1A. Custom crRNA's and tracrRNA's were combined according to the manufacturers' protocol. RNP complexes were made according to the manufacturer's protocol in a 6:1 ratio (gRNA:Cas9 protein). Electroporation was performed on 4 × 10⁵ cells using the Neon transfection system (Thermo Fisher Scientific) with the protocol for SH-Y5Y cells (1200 V, 20 ms pulse, three times).

Clone selection

Transfected cells were seeded with 1000–2500 cells in a 10/15 cm Ø tissue culture plate to form colonies. When colonies reached a size of approximately 5 mm, medium was aspirated and colonies were covered with 8 mm cloning cylinders (Dow Corning) coated in sterile 976V silicone high vacuum grease (Dow Corning) to seal it to the plate. Colonies were subsequently trypsinized and transferred to 96-well plates and grown for further characterization and experiments.

DNA isolation and PCR characterization

DNA was isolated using QuickExtract DNA extract solution (Lucigen) for PCR grade DNA or the QIAamp DNA mini kit (Qiagen) for WGS grade DNA according to the manufacturers' protocols. PCR was performed using Platinum™ II Hot-Start Green PCR Master Mix (Thermo Fisher Scientific). Primers are specified in Table 1B. Sanger sequencing was performed by MacroGen Europe with the same primers used for amplification.

Shallow WGS and bioinformatic analysis

Shallow WGS was performed as described previously (18). In short, library preparation was carried out, comprising fragmentation of DNA by sonication, repair of DNA ends,

3 prime adenylation, adapter ligation, purification, PCR amplification of the fragments with adapters and, lastly, again purification. The Illumina Next Generation Sequencing platform was used for shallow WGS. The sequencing data was analyzed using the QDNAseq R-package (v1.26.0) with default settings and 100 kbp bins (18). Correction for sequence mappability and GC content was carried out, as well as filtering of problematic genomic regions. The R2 bioinformatics platform (R2.amc.nl) and R-Studio (v4.0.2) were used for analysis and visualization.

Karyotyping

Cells were transferred onto Lab-Tek chamber slides (Thermo Fisher Scientific) and grown for 24 h, the last two hours in the presence of colcemid (Thermo Fisher Scientific). After standard cytogenetic harvesting and Giemsa-Trypsin-Giemsa banding 20 metaphase cells were analyzed from the stimulated culture. The karyotypes were described according to ISCN 2016 (19).

RESULTS

Engineering an 11q deletion in neuroblastoma SKNSH cells

Terminal deletions affecting a large part of chromosome 11q are frequently observed in neuroblastoma tumors (14). They occur in 20–40% of patients and are strongly associated with poor survival (Supplementary Figure S1) (20). Loss of 11q is largely mutually exclusive with amplification of the *MYCN* oncogene, the most well-established oncogenic driver in neuroblastoma (21). The high degree of recurrence and link to poor prognosis suggest an oncogenic effect; however, the underlying molecular pathways that drive this effect remain to be elucidated. No recurrently mutated genes have been identified on the remaining copy of 11q, making it unlikely that it serves as the first hit in complete inactivation of a tumor suppressor. Haploinsufficiency of several genes in this region, like *CADMI* and *ATM* (22,23), or microRNAs like the LET-7 microRNA cluster (24), has been suggested as an oncogenic driver of 11q loss. However, this has not led to a consensus on the molecular driving mechanism, let alone therapeutic options to specifically target neuroblastoma tumors with an 11q deletion. Therefore, we aimed to establish an isogenic model of such a deletion in the neuroblastoma cell line SKNSH, which is diploid with two intact copies of chromosome 11 and without *MYCN* amplification (25). We hypothesized that DSBs at two locations, one at chromosome band 11q13.4 and the other at chromosome band 11q25 near the telomere, could lead to joining of the two ends with deletion of the intermediate region. Guide RNAs were designed to induce DSBs within 100 bp of the 11q breakpoint from the neuroblastoma cell line GIMEN, which has lost the terminal regions of 11q through a der(11)t(11;17) (26), and near the telomere on 11q (Figure 1A,B). Joining of these DSBs would induce the same loss of 11q in the cell line SKNSH as observed in the GIMEN cell line, apart from the 11q telomeric region that would remain in SKNSH.

CRISPR and translocation detection. Complexes consisting of Cas9-protein and synthetic gRNA's (Ribo Nucleo

Protein, RNP complexes) were introduced into cells using electroporation. Single RNP complexes have a 60–70% editing efficiency as determined by Inference of CRISPR Edits (ICE) analysis (Synthego Performance Analysis, ICE Analysis. 2019. v2.0. Synthego, Supplementary Figure S2). To facilitate joining of the two DSBs a 100 bp ssDNA molecule consisting of 50 bp stretches of homology to the regions surrounding the DSBs was added to the reaction. To determine whether the desired end-joining took place, PCR was performed on DNA isolated from the bulk transfected cells using primers spanning the expected translocation regions (Figure 2A and Supplementary Figure S3). Gel electrophoresis of the PCR reaction shows bands at the expected size, indicating the presence of a fusion product, while Sanger sequencing confirmed the specificity of the PCR product. Control primers located in close chromosomal proximity confirmed the integrity of the DNA and showed that one wild-type copy of chromosome 11 was still present. Interestingly, the translocation PCR product was not observed when the homologous ssDNA was omitted, indicating that it aids in joining the two DSBs with loss of the intermittent region.

Derivation and characterization of single cell clones. To obtain a homogenous population with the engineered chromosomal loss, after four passages cells were seeded at low density (2000 cells per 10 cm Ø plate) to derive single clones. DNA was subsequently isolated from these clones, and the presence of a translocation product was screened using the previously described PCR strategy. The four first clones that reached a cell density that allowed us to isolate sufficient DNA, all contained a translocation PCR product and Sanger sequencing showed the same sequence for all clones (Figure 2B). However, the sequenced PCR products did not completely match the ssDNA template sequence that would have been expected if the template had been instrumental in the DSB repair. All four clones contained the same 15 bp deletion compared to the anticipated template sequence. Since these cells were cultured for a few passages after electroporation, we concluded that these clones are most likely derived from a common ancestor and are not independent. To determine the reproducibility of the procedure and establish the frequency at which these translocations occur, the 11q deletion engineering experiment was performed again with a new passage of the SKNSH cell line. However, to prevent early outgrowth of positive clones due to possible selective advantages, cells were seeded at lower density (1000 cells per 15 cm Ø plate) 72 h post-electroporation. PCR products spanning the intended fusion were detected in two out of nine clones (Supplementary Figure S4). One of the two positive clones (clone 7) showed a ~350 bp duplication of the 11q13.4 region adjacent to the gRNA recognition site, while the other positive clone (clone 10) showed a 23bp insertion (data not shown), which shows they are of independent origin. Figure 2C shows the PCR verification of the two independent positive clones from this experiment and the positive clone from the previous experiment with two independent primer pairs (A+B and C+D). A third primer pair (A+E) that amplifies a continuous genomic region on chromosome 11 was used as a positive con-

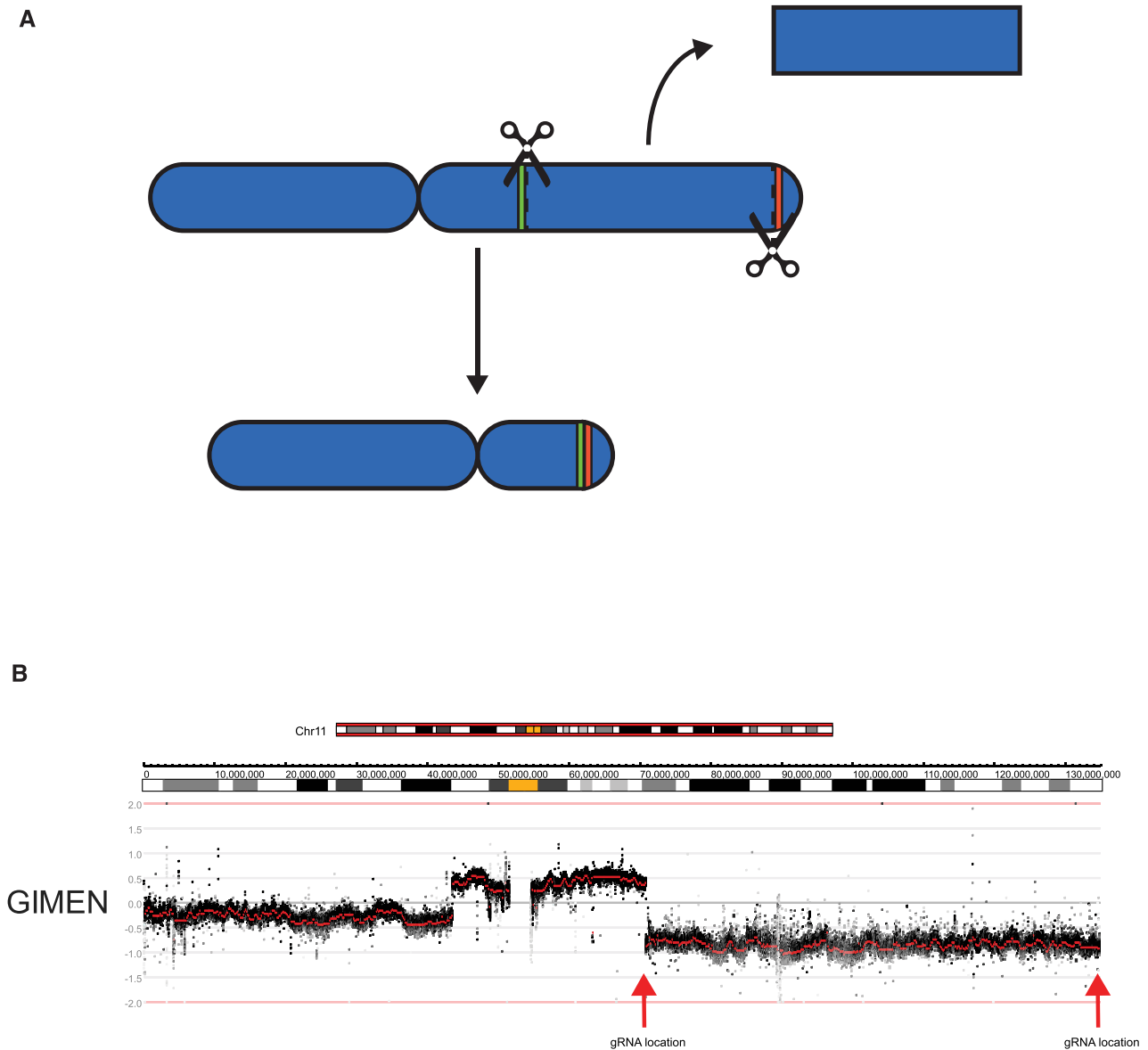


Figure 1. The concept of CRISPR-induced chromosomal deletions. (A) Schematic overview of chromosome 11. Scissors represent the gRNA locations and green and red colors the regions adjacent to the gRNAs. DSBs could lead to joining of the green and red region with loss of the intermittent region. (B) Copy number profile of chromosome 11q of the neuroblastoma cell line GIMEN. Data was generated by WGS and visualized using the R2 bioinformatics platform. Black dots represent values for bins and red dots represent segmented values. The red arrows represent the gRNA location at chromosome 11q13.4 and near the telomere at 11q25. Ideograms representing the chromosomal location and banding pattern (centromeres are represented in yellow) are shown above the profile.

control for the integrity of the wild type DNA and to show that the deletion was heterozygous.

Copy number profiling of clones. To determine if the elected CRISPR-Cas9 approach leads to an 11q deletion of 65 Mb, we used two techniques: (i) karyotyping, which has the power to not only visualize numerical copy number changes genome-wide but also copy number neutral translocations with a resolution of 5–10 Mb and (ii) shallow whole genome sequencing that determines genome-wide copy number aberrations and breakpoints to a resolution of 100 kb. The three clones with a translocation PCR product were analyzed for genome-wide copy number aber-

rations using shallow Whole Genome Sequencing (shallow WGS), together with the wild-type cell line and the three clones that that did not show a translocation PCR product. All three clones with a translocation product showed a clear loss of one copy of the intended region of chromosome 11q, while the other three clones and the wild-type did not show this large-scale loss (Figure 3A and Supplementary Figure S5). Across the entire genome, no additional chromosomal copy number differences were observed for the three PCR positive clones, compared to the PCR negative clones or the parental cell line. Shallow WGS offers a high resolution to detect copy number aberrations, yet translocations cannot be detected. To determine whether no addi-

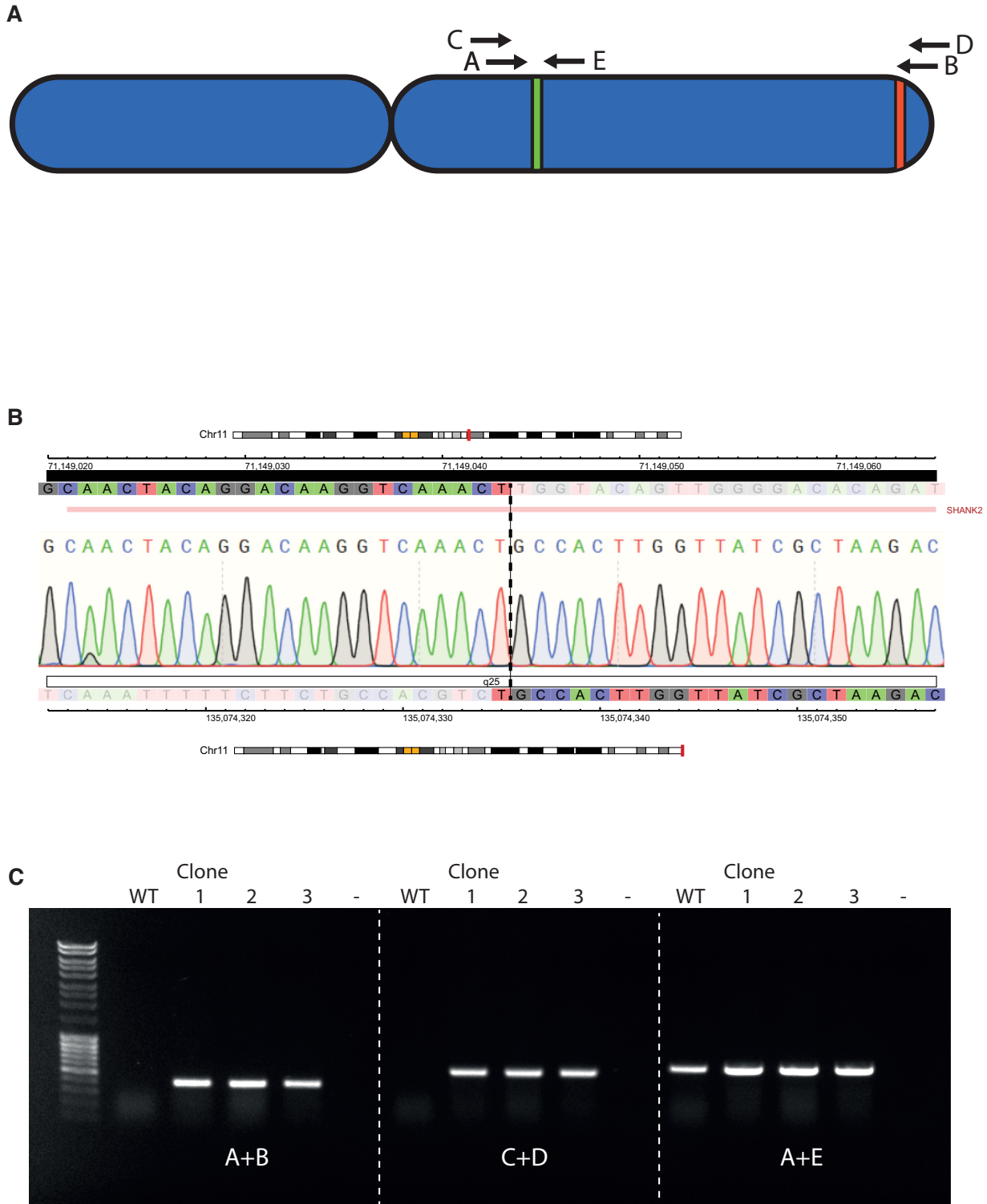


Figure 2. PCR analysis indicates the presence of a translocation between 11q13.4 and 11q25. (A) Schematic overview of chromosome 11, with green and red regions representing the regions adjacent to the gRNA recognition sites and letters representing primers used for analysis. (Table 1A) (B) Sanger sequencing electropherogram results of the translocation product from SKNSH 11q clone 4. Color coded tracks above and below the trace represent the sequence (C = blue, T = red, G = gray, A = green) genomic coordinates (HG19) and chromosomal location of the centromeric and telomeric region of the translocation, respectively. Ideograms representing the chromosomal location (shown in red), banding pattern (centromeres are represented in yellow). The gene located in the affected regions, i.e. the *SHANK2* gene on the centromeric end, is shown above the profile. (C) Agarose gel electrophoresis of the PCR reaction of the wild-type (WT) and the three clones (1, 2 and 3) from two experiments that were positive for the presence of a translocation. The first lane contains Generuler 1 kb DNA ladder (Thermo Fisher Scientific). Primer combinations are shown below the bands and refer to the primers shown in (A).

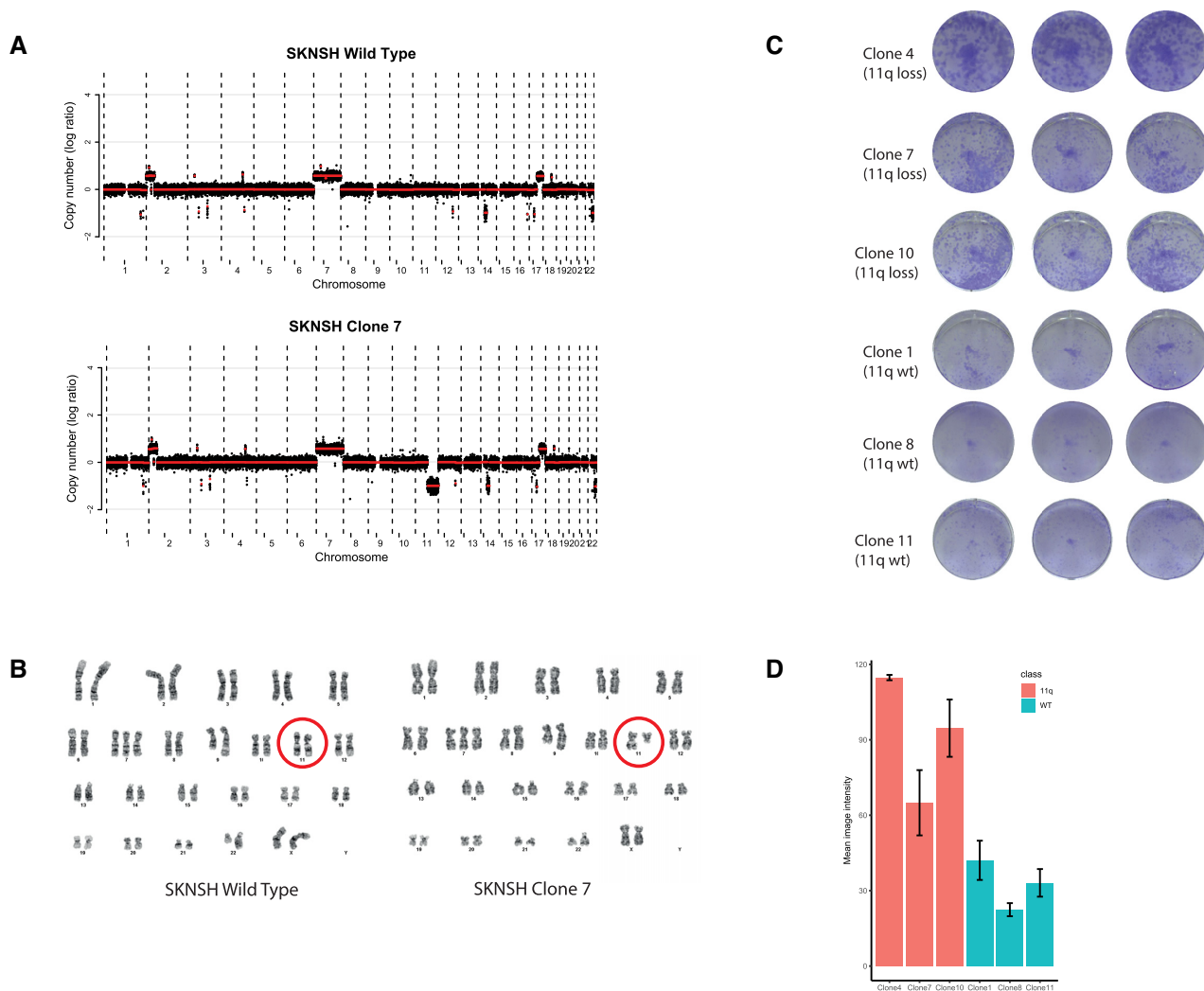


Figure 3. CRISPR induced 11q deletions lead to increased clonogenic capacity in SKNSH. **(A)** Copy number profiles of wild type SKNSH cells and chromosome 11q deletion clone 7 (one of the clones that was positive for the translocation PCR product). The x-axis shows the genomic location and the y-axis shows median-normalized log₂-transformed copy number, with black dots representing bins and red lines representing segmented copy numbers. **(B)** Karyotypes of the wild type cells and chromosome 11q deletion clone 7 cells. Red circles indicate the chromosome 11 pair. Karyotype of the wild-type cell line: 47,X,add(X)(p21.2),+7,add(9)(q34.1),add(22)(q13). Karyotype of the clone: 47,X,add(X)(p21.2),+7,?add(8)(p23),add(9)(q34.1),del(11)(q13),add(22)(q13). **(C)** Crystal violet staining of colony forming assays of three clones with 11q deletion and three clones without. **(D)** Quantification of the experiment shown in (C). Error bars represent the standard deviation of the three wells for each line. Pairwise *t*-test analysis shows significant differences between all chromosome 11q deletion clones and all negative clones.

tional, copy number neutral, translocations occurred due to the CRISPR editing, classical karyotyping was performed for the wild-type parental cell line and PCR positive clone 7. A terminal deletion of chromosome 11 with breakpoint at 11q13 was the only karyotypical difference between this clone and the wild-type (Figure 3B). We conclude that the CRISPR-Cas9 genome editing has indeed caused a translocation between the two regions where DSBs were induced with concomitant deletion of the interstitial region. This cell line, together with the wild-type, represent an isogenic cell line pair that can serve as a model to study the effects of 11q loss in neuroblastoma.

Clonogenic assays. SKNSH clones with chromosome 11q deletions were observed at a high frequency (2/9, 22%) without the use of selection. This led us to hypothesize that

chromosome 11q deletion, observed in 34% of neuroblastoma tumors (14), might give a selective advantage. The SKNSH clones with the translocation were among the first colonies to reach sufficient cells to be harvested for DNA isolation in both experiments (data not shown), suggesting that loss of the long arm of chromosome 11 might cause an increased colony forming capacity. To determine whether this is the case, the same six clones that were characterized by shallow WGS were plated at low density and were stained with crystal violet after 14 days. Clones with 11q deletions showed significantly higher colony forming capacity, as determined by the mean image intensity of the stained wells, than clones that underwent the same procedure but did not show a deletion (Figure 3C, D), suggesting that 11q loss indeed provides an advantage in clonal outgrowth.

Engineering a 6q deletion in neuroblastoma NMB cells

To determine whether this experimental setup is also effective for other chromosomal deletions in other cell lines we aimed to introduce a 6q deletion in the neuroblastoma cell line NMB. Distal 6q loss is observed in ~6% of neuroblastoma patients and is associated with extremely poor prognosis (27) (Supplementary Figure S6). Similar to the 11q experiments, guide RNAs were designed at two locations on chromosome 6q; one at 6q22.1 in close proximity to a rebase specific 6q deletion (26) (Supplementary Figure S7) and the other at 6q27 close to the telomere. Since the ssDNA used in the 11q experiment was possibly not used for repair, as determined by Sanger sequencing, we omitted a ssDNA template from the experimental setup for chromosome 6q. Cells were transfected with the RNP and DNA was isolated from part of the transfected cells. A translocation PCR product was already observed in these bulk transfected cells (Supplementary Figure S8), and single cell clone selection yielded three out of the nine clones positive for such a product (Supplementary Figure S9). Shallow WGS showed a deletion in two of these clones, while one clone with a translocation PCR product and three clones without a translocation product did not show loss of this region (Figure 4A and Supplementary Figure S10). Three clones that did not show a translocation PCR product did not show loss of chromosome 6q. In general, it becomes clear that the clones, both with- and without a 6q deletion, have a very different chromosomal make-up. They show major differences in copy numbers of chromosomes other than 6q and even apparent ploidy changes (Figure 4B and Supplementary Figure S11). Whether this genomic instability is the result of the CRISPR-Cas9 editing or is inherent to the cell line used remains to be determined. Notwithstanding, the described CRISPR procedure allows for a fast and efficient targeted deletion, also for chromosome 6q.

In conclusion, we have successfully developed a procedure to efficiently induce large chromosomal deletions in neuroblastoma cell lines using CRISPR-Cas9. It is reasonable to assume that this method will be applicable to other cancer types and other chromosomes which would enable the rapid generation of isogenic cell models that would allow the study of molecular mechanisms that drive clinically relevant chromosomal deletions.

DISCUSSION

Recurrent large-scale chromosomal copy number aberrations are observed in almost all cancer types and are often associated with poor prognosis (28,29). Despite the observation that the most recurrent events occur at similar frequencies as the most frequently mutated gene, TP53 (30), and more frequently than the most frequent focal copy number aberrations (1), their molecular effects have been far less studied and consequently less understood. Therefore, we devised a strategy to induce large-scale chromosomal deletions using CRISPR-Cas9 by introducing DSBs at known breakpoints and telomeric regions and providing a ssDNA template for repair. The presented method is easy and fast, and we observed high frequencies with >30% of clones with the intended chromosomal deletion.

Recently, three alternative methods have been described that also enable the modelling of large chromosomal rearrangements. CRISPR-Cas9 has already been employed to fuse two DSBs on two different chromosomes together for the generation of a fusion gene. However, here a selectable marker was used to select cells with the designed fusion and no copy number aberrations were involved (31). In another study, TALENs were used to engineer a chromosome 8p deletion in breast cancer cells (32). This approach was very similar to ours, apart from the use of TALENs instead of CRISPR-Cas9 technology. Finally, CRISPR-Cas9 was used to delete chromosome 3p in lung cells; however, here DSBs were induced near the centromere, but combined with an artificial telomere plasmid with a selectable marker (8). The advantage of our method is that no molecular cloning is involved, since all reagents can be designed *in silico* and readily ordered, making it cheaper and faster than the alternative methods. Moreover, no exogenous DNA sequences are introduced into the genome of these cells, which makes it a more isogenic model system.

We observe clones positive for the intended chromosomal deletions at high frequency (over 30%), although these frequencies may be imprecise due to the low amount of analyzed clones. Even though the editing efficiencies of the single gRNAs observed were as high as 60%, we would regard these frequencies as improbable without a positive selective effect of the induced deletions on the growth and selection of these colonies for PCR evaluation. In line with this, for chromosome 11q loss in the neuroblastoma cell line SKNSH we observe an increase in colony forming capacity in the 11q deletion clones compared to clones without the 11q deletion. This also explains why the first colonies that had grown to sufficient cell numbers for PCR evaluation contained the intended deletions. This positive effect on the growth of this cell line is contrary to earlier results where chromosomal deletions were induced (8,32), where no or little positive effect on proliferation was observed. One key difference is, however, that we use established cancer cells while in these studies karyotypically normal cells were used. It is conceivable that cancer cells already fulfill some of the requirements, i.e. reduced genome maintenance or other hallmarks of cancer (28), that allow the positive effect of these deletions to manifest itself. If no strong growth advantage of the projected deletion is expected a selectable marker could be added to the ssDNA, or plasmid DNA with homology arms and a selection marker could be used as a repair template. However, it remains to be determined whether it is possible to induce these large-scale deletions in nontransformed models such as human primary cells or mouse models, since they are generally much less tolerant to aneuploidy (33). Moreover, we hypothesize that a suitable genetic background, i.e. taking into account mutual exclusivity, cell subtype etc., is also a prerequisite for the efficient induction of these large-scale deletions.

In our initial experimental set-up for chromosome 11q, we used a ssDNA template containing homology regions of both locations where DSBs were induced, since it has been suggested that such templates aid in driving repair through homologous recombination (34) and a double strand DNA template would be more prone to lead to off-target insertions or cytotoxic side effects in the transfected cells

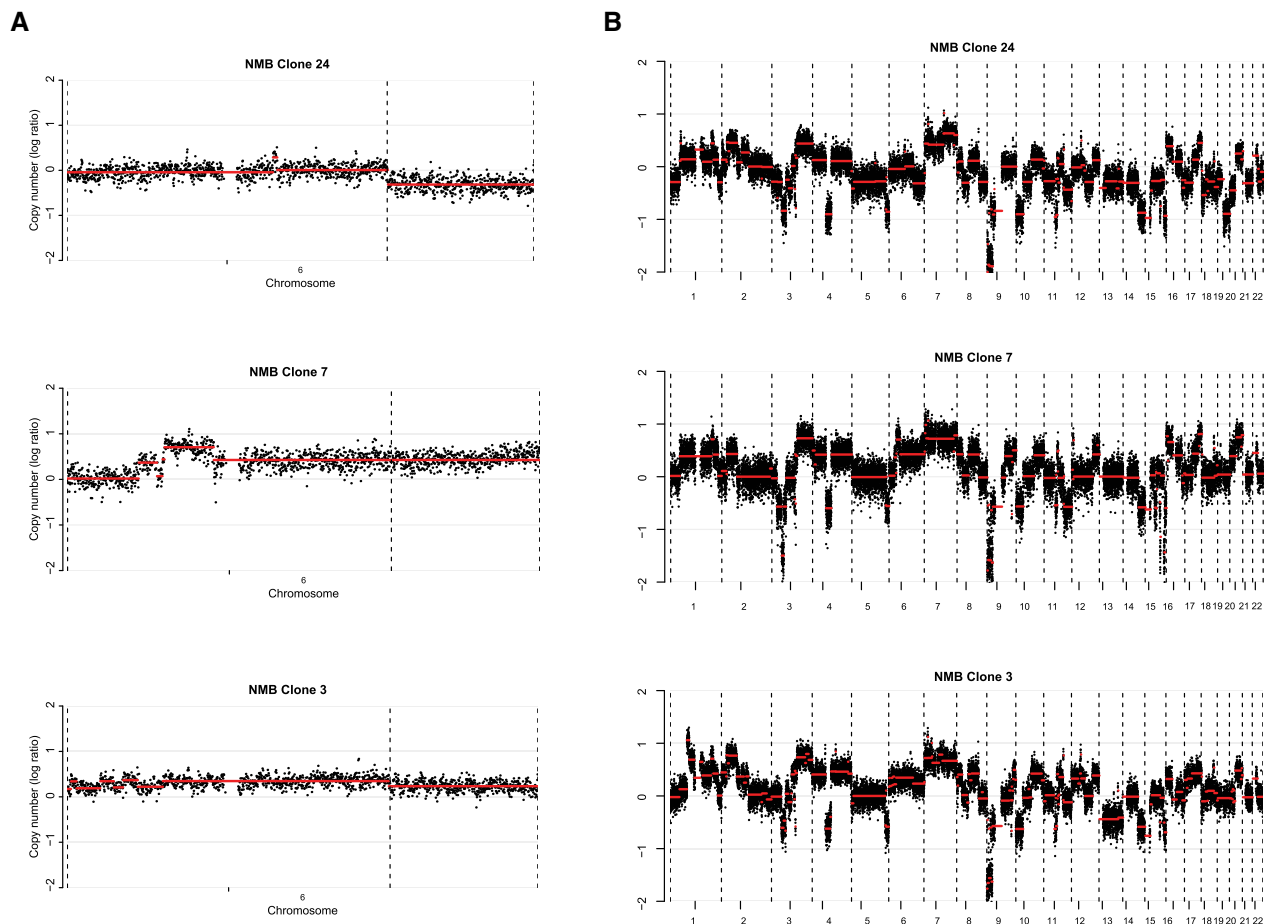


Figure 4. Chromosome 6q deletion and genomic heterogeneity in the cell line NMB. (A) Copy number profiles of chromosome 6 of the three clones that were positive for a translocation PCR product. The *x*-axis shows the genomic location, and the *y*-axis shows median-normalized \log_2 -transformed copy number, with black dots representing bins and red lines representing segmented copy numbers. Clone 24 and 3 show a deletion on 6q, while this is not observed in clone 7. (B) Whole genome overview of the copy numbers of the three clones that were positive for a translocation PCR product. The *x*-axis shows the genomic location, and the *y*-axis shows median-normalized \log_2 -transformed copy number, with black dots representing bins and red lines representing segmented copy numbers.

(35). We did observe PCR products suggestive of successful translocations in the cells where a ssDNA template was added, while these were not observed in cells without this template. However, Sanger sequencing analysis of single cell clones that showed such a product (and later showed to have acquired the 11q loss) yielded sequences that showed deletions or duplications compared to the ssDNA sequence. It is thought that ssDNA aids in the repair of DSBs through homologous recombination, which is generally considered to be an error-free process (36), although this concept has been challenged (37). The ssDNA templates were omitted in experiments where 6q loss was induced; however, we also observed relatively high frequencies of the intended translocation in these experiments, suggesting that ssDNA templates are not absolutely necessary to join the two DSBs. More research is necessary to determine whether ssDNA templates contribute to successful generation of these deletions and to what extent.

Although CRISPR-Cas9 can be used to induce DSBs at specific locations, it has been known to also produce unintended effects on chromosomal make-up (38,39). In the

11q CRISPR clones of the cell line SKNSH, we do not observe additional large chromosomal changes, apart from the intended 11q deletion. There could be small structural changes or single nucleotide variants that we were unable to detect; however, it seems unlikely that these play a role in the observed increase in clonogenic capacity, since independently derived clones showed the same phenotype. For the cell line NMB, we see a very different pattern with a lot of chromosomal changes besides the intended 6q. It has been established that CRISPR-Cas9 can also cause unintended chromosomal rearrangements and overall changes in ploidy and chromosome number (39). The observed chromosomal changes could reflect the genetic heterogeneity of the NMB cell line, which may be amplified by the clonal selection step in the procedure; however, they could also be unintended side-effects of CRISPR-Cas9 treatment.

In conclusion, we show that it is feasible to engineer large-scale chromosomal deletions in a fast and efficient fashion while maintaining the original telomere and without the introduction of exogenous DNA sequences. For the deletion of 11q in the neuroblastoma cell line SKNSH an effect on

colony formation was readily observed, which could suggest activation of specific oncogenic pathways. Many studies have addressed potential target genes that confer the oncogenic effect of 11q loss in neuroblastoma (40); however, this approach has largely failed to elucidate the underlying mechanism or to identify treatment options. Creating isogenic cell lines for chromosomal deletions will obviate this gene-by-gene approach and enable researchers to directly study molecular effects and possible associated therapies with a chromosomal rather than just gene-oriented approach.

DATA AVAILABILITY

Shallow WGS data is available at EGA (accession nr. EGAS00001005134).

SUPPLEMENTARY DATA

Supplementary Data are available at NAR Online.

ACKNOWLEDGEMENTS

We would like to thank Prof. Jan Molenaar for supplying the neuroblastoma cell lines and Dr. Erik van Dijk for assistance with the analysis of the shallow whole genome sequencing data.

FUNDING

Dutch Cancer Society [KWF 20161-1-10271]. Funding for open access charge: KWF Kankerbestrijding.
Conflict of interest statement. None declared.

REFERENCES

1. Beroukhi, R., Mermel, C.H., Porter, D., Wei, G., Raychaudhuri, S., Donovan, J., Barretina, J., Boehm, J.S., Dobson, J., Urashima, M. *et al.* (2010) The landscape of somatic copy-number alteration across human cancers. *Nature*, **463**, 899–905.
2. Chapman, P.B., Hauschild, A., Robert, C., Haanen, J.B., Ascierto, P., Larkin, J., Dummer, R., Garbe, C., Testori, A., Maio, M. *et al.* (2011) Improved survival with vemurafenib in melanoma with BRAF V600E mutation. *N. Engl. J. Med.*, **364**, 2507–2516.
3. Druker, B.J., Tamura, S., Buchdunger, E., Ohno, S., Segal, G.M., Fanning, S., Zimmermann, J. and Lydon, N.B. (1996) Effects of a selective inhibitor of the Abl tyrosine kinase on the growth of Bcr-Abl positive cells. *Nat. Med.*, **2**, 561–566.
4. Krijgsman, O., Carvalho, B., Meijer, G.A., Steenbergen, R.D. and Ylstra, B. (2014) Focal chromosomal copy number aberrations in cancer—Needles in a genome haystack. *Biochim. Biophys. Acta*, **1843**, 2698–2704.
5. Zack, T.I., Schumacher, S.E., Carter, S.L., Cherniack, A.D., Saksena, G., Tabak, B., Lawrence, M.S., Zhsng, C.Z., Wala, J., Mermel, C.H. *et al.* (2013) Pan-cancer patterns of somatic copy number alteration. *Nat. Genet.*, **45**, 1134–1140.
6. Varambally, S., Cao, Q., Mani, R.S., Shankar, S., Wang, X., Ateeq, B., Laxman, B., Cao, X., Jing, X., Ramnarayanan, K. *et al.* (2008) Genomic loss of microRNA-101 leads to overexpression of histone methyltransferase EZH2 in cancer. *Science (New York, N. Y.)*, **322**, 1695–1699.
7. Slamon, D.J., Leyland-Jones, B., Shak, S., Fuchs, H., Paton, V., Bajamonde, A., Fleming, T., Eiermann, W., Wolter, J., Pegram, M. *et al.* (2001) Use of chemotherapy plus a monoclonal antibody against HER2 for metastatic breast cancer that overexpresses HER2. *N. Engl. J. Med.*, **344**, 783–792.
8. Taylor, A.M., Shih, J., Ha, G., Gao, G.F., Zhang, X., Berger, A.C., Schumacher, S.E., Wang, C., Hu, H., Liu, J. *et al.* (2018) Genomic and functional approaches to understanding cancer aneuploidy. *Cancer Cell*, **33**, 676–689.
9. Pollack, J.R., Sørlie, T., Perou, C.M., Rees, C.A., Jeffrey, S.S., Lonning, P.E., Tibshirani, R., Botstein, D., Børresen-Dale, A.L. and Brown, P.O. (2002) Microarray analysis reveals a major direct role of DNA copy number alteration in the transcriptional program of human breast tumors. *Proc. Natl. Acad. Sci. USA*, **99**, 12963–12968.
10. Ried, T., Hu, Y., Difilippantonio, M.J., Ghadimi, B.M., Grade, M. and Camps, J. (2012) The consequences of chromosomal aneuploidy on the transcriptome of cancer cells. *Biochim. Biophys. Acta*, **1819**, 784–793.
11. Sheltzer, J.M., Ko, J.H., Replogle, J.M., Habibe Burgos, N.C., Chung, E.S., Meehl, C.M., Sayles, N.M., Passerini, V., Storchova, Z. and Amon, A. (2017) Single-chromosome gains commonly function as tumor suppressors. *Cancer Cell*, **31**, 240–255.
12. Williams, B.R., Prabhu, V.R., Hunter, K.E., Glazier, C.M., Whittaker, C.A., Housman, D.E. and Amon, A. (2008) Aneuploidy affects proliferation and spontaneous immortalization in mammalian cells. *Science (New York, N. Y.)*, **322**, 703–709.
13. Molenaar, J.J., Koster, J., Zwijnenburg, D.A., van Sluis, P., Valentijn, L.J., van der Ploeg, I., Hamdi, M., van Nes, J., Westerman, B.A., van Arkel, J. *et al.* (2012) Sequencing of neuroblastoma identifies chromothripsis and defects in neurogenesis genes. *Nature*, **483**, 589–593.
14. Attiyeh, E.F., London, W.B., Mossé, Y.P., Wang, Q., Winter, C., Khazi, D., McGrady, P.W., Seeger, R.C., Look, A.T., Shimada, H. *et al.* (2005) Chromosome 1p and 11q deletions and outcome in neuroblastoma. *N. Engl. J. Med.*, **353**, 2243–2253.
15. Bown, N., Cotterill, S., Lastowska, M., O’Neill, S., Pearson, A.D., Plantaz, D., Meddeb, M., Danglot, G., Brinkschmidt, C., Christiansen, H. *et al.* (1999) Gain of chromosome Arm 17q and adverse outcome in patients with neuroblastoma. *N. Engl. J. Med.*, **340**, 1954–1961.
16. Rinehart, T.A. (2004) AFLP analysis using GeneMapper software and an Excel macro that aligns and converts output to binary. *BioTechniques*, **37**, 186–188.
17. Schneider, C.A., Rasband, W.S. and Eliceiri, K.W. (2012) NIH Image to ImageJ: 25 years of image analysis. *Nat. Methods*, **9**, 671–675.
18. Scheinin, I., Sie, D., Bengtsson, H., van de Wiel, M.A., Olshen, A.B., van Thuijl, H.F., van Essen, H.F., Eijk, P.P., Rustenburg, F., Meijer, G.A. *et al.* (2014) DNA copy number analysis of fresh and formalin-fixed specimens by shallow whole-genome sequencing with identification and exclusion of problematic regions in the genome assembly. *Genome Res.*, **24**, 2022–2032.
19. International Standing Committee on Human Cytogenetic, N., Simons, A., McGowan-Jordan, J. and Schmid, M. (2016) In: *ISCN 2016: An International System for Human Cytogenetic Nomenclature (2016)*. Karger, Basel.
20. Kumps, C., Fieuw, A., Mestdagh, P., Menten, B., Lefever, S., Pattyn, F., De Brouwer, S., Sante, T., Schulte, J.H., Schramm, A. *et al.* (2013) Focal DNA copy number changes in neuroblastoma target MYCN regulated genes. *PLoS One*, **8**, e52321.
21. Guo, C., White, P.S., Weiss, M.J., Hogarty, M.D., Thompson, P.M., Stram, D.O., Gerbing, R., Matthay, K.K., Seeger, R.C., Brodeur, G.M. *et al.* (1999) Allelic deletion at 11q23 is common in MYCN single copy neuroblastomas. *Oncogene*, **18**, 4948–4957.
22. Mandriota, S.J., Valentijn, L.J., Lesne, L., Betts, D.R., Marino, D., Boudal-Khoshbeen, M., London, W.B., Rougemont, A.L., Attiyeh, E.F., Maris, J.M. *et al.* (2015) Ataxia-telangiectasia mutated (ATM) silencing promotes neuroblastoma progression through a MYCN independent mechanism. *Oncotarget*, **6**, 18558–18576.
23. Michels, E., Hoebeek, J., De Preter, K., Schramm, A., Brichard, B., De Paepe, A., Eggert, A., Laureys, G., Vandesompele, J. and Speleman, F. (2008) CADM1 is a strong neuroblastoma candidate gene that maps within a 3.72 Mb critical region of loss on 11q23. *BMC Cancer*, **8**, 173.
24. Powers, J.T., Tsanov, K.M., Pearson, D.S., Roels, F., Spina, C.S., Ebright, R., Seligson, M., de Soysa, Y., Cahan, P., Theifßen, J. *et al.* (2016) Multiple mechanisms disrupt the let-7 microRNA family in neuroblastoma. *Nature*, **535**, 246–251.
25. Kim, G.J., Park, S.Y., Kim, H., Chun, Y.H. and Park, S.H. (2001) Chromosomal aberrations in neuroblastoma cell lines identified by

- cross species color banding and chromosome painting. *Cancer Genet. Cytogenet.*, **129**, 10–16.
26. Eleveld, T.F., Oldridge, D.A., Bernard, V., Koster, J., Colmet Daage, L., Diskin, S.J., Schild, L., Bentahar, N.B., Bellini, A., Chicard, M. *et al.* (2015) Relapsed neuroblastomas show frequent RAS-MAPK pathway mutations. *Nat. Genet.*, **47**, 864–871.
 27. Depuydt, P., Boeva, V., Hocking, T.D., Cannoodt, R., Ambros, I.M., Ambros, P.F., Asgharzadeh, S., Attiyeh, E.F., Combaret, V., Defferrari, R. *et al.* (2018) Genomic amplifications and distal 6q Loss: Novel markers for poor survival in high-risk neuroblastoma patients. *J. Natl. Cancer Inst.*, **110**, 1084–1093.
 28. Hanahan, D. and Weinberg, R.A. (2011) Hallmarks of cancer: the next generation. *Cell*, **144**, 646–674.
 29. Macintyre, G., Ylstra, B. and Brenton, J.D. (2016) Sequencing structural variants in cancer for precision therapeutics. *Trends Genet.*, **32**, 530–542.
 30. Donehower, L.A., Soussi, T., Korkut, A., Liu, Y., Schultz, A., Cardenas, M., Li, X., Babur, O., Hsu, T.K., Lichtarge, O. *et al.* (2019) Integrated analysis of TP53 gene and pathway alterations in the cancer genome atlas. *Cell Rep.*, **28**, 1370–1384.
 31. Vanoli, F., Tomishima, M., Feng, W., Lamribet, K., Babin, L., Brunet, E. and Jasin, M. (2017) CRISPR-Cas9-guided oncogenic chromosomal translocations with conditional fusion protein expression in human mesenchymal cells. *Proc. Natl. Acad. Sci. USA*, **114**, 3696–3701.
 32. Cai, Y., Crowther, J., Pastor, T., Abbasi Asbagh, L., Baietti, M.F., De Troyer, M., Vazquez, I., Talebi, A., Renzi, F., Dehairs, J. *et al.* (2016) Loss of Chromosome 8p Governs Tumor Progression and Drug Response by Altering Lipid Metabolism. *Cancer Cell*, **29**, 751–766.
 33. Sansregret, L. and Swanton, C. (2017) The role of aneuploidy in cancer evolution. *Cold Spring Harb. Perspect. Med.*, **7**, a028373.
 34. Paquet, D., Kwart, D., Chen, A., Sproul, A., Jacob, S., Teo, S., Olsen, K.M., Gregg, A., Noggle, S. and Tessier-Lavigne, M. (2016) Efficient introduction of specific homozygous and heterozygous mutations using CRISPR/Cas9. *Nature*, **533**, 125–129.
 35. Roth, T.L., Puig-Saus, C., Yu, R., Shifrut, E., Carnevale, J., Li, P.J., Hiatt, J., Saco, J., Krystofinski, P., Li, H. *et al.* (2018) Reprogramming human T cell function and specificity with non-viral genome targeting. *Nature*, **559**, 405–409.
 36. Helleday, T. (2010) Homologous recombination in cancer development, treatment and development of drug resistance. *Carcinogenesis*, **31**, 955–960.
 37. Guirouilh-Barbat, J., Lambert, S., Bertrand, P. and Lopez, B.S. (2014) Is homologous recombination really an error-free process? *Front. Genet.*, **5**, 175.
 38. Cullot, G., Boutin, J., Toutain, J., Prat, F., Pennamen, P., Rooryck, C., Teichmann, M., Rousseau, E., Lamrissi-Garcia, I., Guyonnet-Duperat, V. *et al.* (2019) CRISPR-Cas9 genome editing induces megabase-scale chromosomal truncations. *Nat. Commun.*, **10**, 1136.
 39. Rayner, E., Durin, M.A., Thomas, R., Moralli, D., O’Cathail, S.M., Tomlinson, I., Green, C.M. and Lewis, A. (2019) CRISPR-Cas9 causes chromosomal instability and rearrangements in cancer cell lines, detectable by cytogenetic methods. *CRISPR J.*, **2**, 406–416.
 40. Mlakar, V., Jurkovic Mlakar, S., Lopez, G., Maris, J.M., Ansari, M. and Gummy-Pause, F. (2017) 11q deletion in neuroblastoma: a review of biological and clinical implications. *Mol. Cancer*, **16**, 114.